Available online at www.sciencedirect.com
SCIENCE DIRECT®
Catalysis Today 90 (2004) 27–34
CATALYSIS TODAY
www.elsevier.com/locate/cattod

From three-way to deNO$_x$ catalysis: a general model

Gérald Djéga-Mariadassou*

Laboratoire Réactivité de Surface CNRS UMR 7609, Université Pierre et Marie Curie, 4 Place Jussieu, 75252 Paris Cedex 05, France

Received 4 September 2003; received in revised form 27 February 2004; accepted 25 March 2004

Available online 15 June 2004

Abstract

A general model is proposed for investigating catalytic sequences from "three-way catalysis" (TWC) to "deNO$_x$" reactions, including plasma-assisted deNO$_x$ processes. This presentation classifies the various NO$_x$ reduction processes, according to the amount of oxygen in the feed (stoichiometric or lean conditions) and, consequently, to the nature of active sites. The model deals with both zero-valent (M^0), mainly for TWC, and cationic (M^{x+}) transition metal (TM) active sites, for both TWC and deNO$_x$ reactions. For anyone of the above processes, the basis of the model assumes that scissions of nitrogen–oxygen bonds occur, leading to the formation of N$_2$, and leaving oxygen species strongly adsorbed on the active site. In the case of TWC and stoichiometric conditions, a catalytic coupling occurs between NO decomposition and CO oxidation in the same catalytic cycle, over both M^0 and M^{x+}. In lean conditions, the deNO$_x$ process in the presence of TM cations needs three kinetically uncoupled functions and, therefore, three catalytic cycles which have to turn over simultaneously. The formation and role of organo-nitro compounds, in one of the three catalytic sequences, seem to be obvious, according to the model. From TWC to deNO$_x$ processes, N$_2$O is the surface intermediate leading to dinitrogen.

Keywords: Zero-valent or cationic TM; Catalytic coupling in TWC; Three uncoupled functions in deNO$_x$ process; Plasma assisted deNO$_x$ process

1. Introduction

Much of published work on emission control for lean-burn engines has been reviewed [1–4]. In one of these recent reviews of the selective reduction of NO$_x$ with hydrocarbons under lean-burn conditions, Burch et al. [4] have concluded that "direct and efficient NO$_x$ reduction catalysts may be very difficult to discover". For these authors, the main problems are related to complex real exhaust emissions, different contact times used between laboratories and engine tests, and temperature range which is wider for an engine test than for a laboratory one.

In the present paper, we shall start from the conclusions of Burch et al. [4], and emphasise two other parameters which seem to be very important:

(i) The oxidation state of the transition metal (TM)

In the case of three-way catalysts (TWC), there is a general agreement for the kinetics of CO oxidation (one of the reaction in TWC) over Rh^0 single crystals [5], and Rh^0/SiO$_2$ [6,7], whereas conclusions are rather controversial for Rh in the presence of CeO$_2$ [8–10] or Rh/Ce-ZrO$_2$. The nature of the catalytic TM site seems to be unclear in a great number of published papers. Nevertheless, in our group, Fajardie et al. have shown, by kinetic measurements, that 100% of Rh^{x+} over Rh/CeO$_2$ (75%)-ZrO$_2$ (25%) catalysts can exist in a stable form [11], whereas Salin et al. have found that Rh/SiO$_2$ catalysts exhibit 100% of Rh [12]. In commercial catalysts both kinds of sites are present and we have described a method for titrating each of them [12].

(ii) The role of organo–nitro compounds as intermediates in the formation of N$_2$

The hydrocarbon activation is very crucial in the lean-deNO$_x$ reaction. According to Burch et al. [4] "the key question is whether these specific organic-type intermediates would be formed under lean deNO$_x$ conditions and this is still not confirmed". To complete this conclusion we have to add that when organo–nitro compounds become reactive with temperature (higher associated rate constant when temperature is rising), then their concentration may become very low in the gas phase at the outlet of the reactor: intermediates react

* Tel.: +33-14-4273624; fax: +33-14-4276033.
E-mail address: djega@ccr.jussieu.fr (G. Djéga-Mariadassou).

0920-5861/$ – see front matter © 2004 Elsevier B.V. All rights reserved.
doi:10.1016/j.cattod.2004.04.004

and have no chance for desorbing before transforming. Furthermore, we shall see later that organo–nitro compounds are intermediates which probably do not lead directly to the formation of N_2. In a future work, we shall see it is easy to detect them by the products of their decomposition.

This paper reports the results from transient experiments (mainly temperature programmed desorption (TPD) or surface reaction (TPSR)), coupled with online analysis of the reaction mixture at the outlet of a well-stirred reactor. It means that the gas composition detected at the outlet of the reactor is that in contact with the catalyst inside the reactor. A "step-by-step" methodology of the main events is described. The role of NO_2, reductant, organo–nitro compounds, N_2O and the formation of N_2 will be considered. This methodology results in a general model of the "global" reduction of NO by a reductant: CO for TWC, and hydrocarbons or partially oxidised species (depending on the process), for deNO$_x$, assisted, or not, by plasma. The present model should integrate the investigation of hundreds of catalyst formulations, as well as previous models and theories. In the case of deNO$_x$ reactions (lean conditions), the present model is based on "three-function catalysts" [13,14,21]. If one function is not efficient or missing, the material will not work properly. The corresponding three catalytic cycles should have to turn over simultaneously. The model should provide a good approach for a final catalyst design.

2. Basic elementary steps of TWC and deNO$_x$ processes

Let us recall that TWC can occur over both M^0 or M^{x+}, whereas deNO$_x$ (lean conditions) mainly occurs over M^{x+} catalytic sites. Nevertheless M^0 can also be considered in the case of deNO$_x$.

At this level, two catalytic processes can be therefore considered, depending on the oxidation state of the transition metal.

Table 1 summarises the basis previously presented by Djéga-Mariadassou et al. [15], on NO decomposition assisted by CO over reduced or oxidised rhodium species supported on ceria. For anyone of the "global" reductions of NO to N_2 (Table 1), the model assumes that scissions of nitrogen–oxygen bonds occur, leading to the formation of N_2, and leaving oxygen species strongly adsorbed on the active site:

$$2NO + 2^* = N_2 + 2^*O \quad (1)$$

$$2NO + 1\cdot = N_2 + O\cdot O \quad (1')$$

where "$*$" or "$\cdot$", and "*O" or "O·O", stand for free active sites M^0, M^{n+} and adsorbed oxygen species, respectively. The symbol "=" means that Eqs. (1) and (1′) represent "global" reactions, not elementary steps [16,17]. It also means that, in all cases, NO decomposition or "global reduction" to N_2 goes through:

Table 1
Main elementary steps and features of the general model for the NO reduction to N_2 over M^0 (TWC or deNO$_x$) and M^{n+} (TWC or deNO$_x$)

Zero-valent metal: $M^0(*)$	Metal cation: $M^{n+}(\cdot)$
(A) NO dissociative adsorption $* + NO \rightleftarrows {}^*NO$, ${}^*NO + * \rightleftarrows {}^*N + {}^*O$	NO associative adsorption $\cdot + 2NO \rightleftarrows NO\cdot NO$ (homogeneous supported catalysis, NO being a ligand)
(B) "N_2 formation" ${}^*N + {}^*N \rightarrow N_2 + 2^*$ (previous *O remain adsorbed and inhibit the active site)	$NO\cdot NO \rightarrow N_2O\cdot O$, $N_2O\cdot O \rightarrow O\cdot O + N_2$ (the O · O species inhibits the reaction)
(C) "O_{ads}" species scavenging In both M^0 and M^{n+} cases, the system needs a reductant to "regenerate" the active site: CO in the case of a stoichiometric mixture (TWC) Activated hydrocarbon (HC) in lean conditions (deNO$_x$)	

- the adsorption of, at least, two NO molecules;
- the dissociation of 2NO leaving 2O$_{ads}$;
- the necessity, for a reductant, to scavenge the 2O$_{ads}$, for recovering the free sites and permitting the reaction to turn over.

This model is in agreement with Burch et al.'s conclusion [4]: "So far, none of these [bibliographical] experimental results seem to exclude NO dissociation as a critical process in the lean deNO$_x$ reaction on PGMs (platinum group metals)". We can generalise to TWC.

Let us note, in the case of lean-burn conditions (deNO$_x$), that "organo–nitro compounds" (RNO$_x$) are not considered, in the model, as directly leading to N_2, in contrast to the assumption of Jayat et al. [18]. This point will be justified hereafter by the assumption of multi-function catalysts in the case of the deNO$_x$ reaction. It does not mean they are not existing (see function 2 of the model), but they do not directly lead to N_2, which occurs on another site (see the third function of the model).

In our model, the formation of N_2O is also included, as the main intermediate of NO decomposition to N_2. But its formation does not follow the same elementary steps, depending on the oxidation state of the metal [15].

In the NO dissociative adsorption on a zero-valent metal (Table 1, case A), two elementary steps for NO chemisorption-dissociation are needed. (Let us note the same two steps are also required for the O_2 adsorption–dissociation process in CO oxidation [17].) This can be explained by the high oxygen coverage in both TWC [19] and lean deNO$_x$ [4] conditions. Therefore, it means that when NO sticks to the surface, it cannot find the two adjacent sites required for its dissociation. Then N_2O can form when *NO and *N are adjacent. These events are consistent with some of the elementary steps described in the

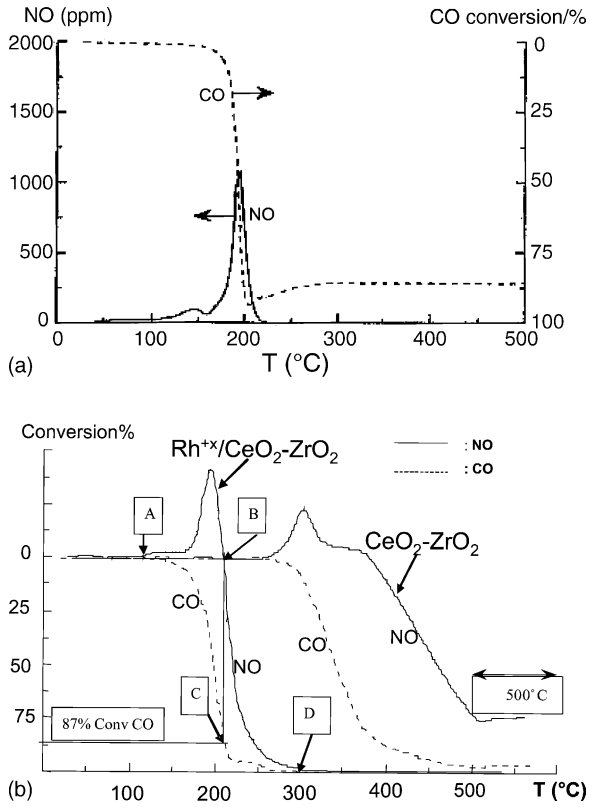

Fig. 1. (a) TPD of NO under a flowing mixture (CO–O_2 (1.5 vol.% CO + 0.65 vol.% O_2 + He (concentrations equivalent to TWC conditions), 180 °C h^{-1}, 5 L h^{-1})) [27]. The Rh^{x+}/CeO_2-ZrO_2 catalyst has been pre-treated first by TPSR in a stoichiometric mixture (1.5 vol.% CO, 0.2 vol.% NO, 0.65 vol.% O_2 in He), then exposed to this mixture at room temperature before TPD. (b) Comparison between CeO_2-ZrO_2 and Rh^{x+}/CeO_2-ZrO_2 in the reduction of NO by CO in the above TWC conditions [27].

dissociation–reduction "mechanism" of Burch et al. [4,20] (zero-valent metal).

But it generally seems that confusion exists between M^0 and M^{x+}. It more particularly brings contradictory conclusions in the formation of N_2O, due to the fact that the catalytic sequence is not the same on M^0 and M^{x+} sites [15].

The very important and interesting point, in both TWC and deNO_x processes, is the simultaneous activation of NO(ads) and reductant(ads) as evidenced by transient temperature programmed reactions (see hereafter Figs. 1 and 5), leading to the "assisted" reduction of NO by this reductant. We never have a direct interaction between NO and the reductant, but rather two main steps: decomposition of NO and oxygen-scavenging by the reductant.

3. Experimental

3.1. Three-way catalysis

$CO/NO/O_2$ reactions were performed at atmospheric pressure in a dynamic flow microreactor. Kinetic studies were carried out in a U-type quartz reactor (8 mm i.d.) where reactant gases were fed from independent mass flow controllers. The reactor outflow was analysed on-line using both a CO infrared detector (Maihak Finor) and a gas chromatograph (HP 5890) equipped with a two packed-column system (Porapak Q and Gas chrom MP-1) and a thermal conductivity detector. All catalytic runs were performed after a pre-treatment of catalysts in flowing hydrogen at 773 K. The catalytic activities of the samples were characterised in the $CO/NO/O_2$ reactions in temperature programmed experiments from 298 to 773 K (light-off conditions) at a constant heating rate of 453 K h^{-1}, with a space velocity from 90 to 125,000 h^{-1}. The feed stream (15 L h^{-1}) consisted of a stoichiometric gas mixture containing 1.5 vol.% CO, 0.20 vol.% NO, and 0.65 vol.% O_2 in helium, the composition of which being monitored by mass flowmeters. The catalyst sample (200 mg) was placed in an oven whose heating rate was monitored by a West 2050 programmator. In these conditions, the reactor behaves like a continuous stirred reactor (CSTR). Continuous analysis of the gas mixture at the inlet and at the outlet of the reactor was performed by a Maihak Finor infrared detector for CO, a Thermoelectron chemiluminescent NO/NO_x analyser for NO, and by gas chromatography to control the eventual presence of N_2O in the effluents. Experimental data were given as conversion versus temperature plots allowing the determination of the temperature of light-off (50% conversion) of reactants.

3.2. deNO_x reaction in lean conditions

The catalytic activity was measured at atmospheric pressure in a fixed-bed flow U-type quartz reactor. During the temperature programmed surface reaction (TPSR) experiment, the reactant concentrations were 150 ppm NO, 8% O_2, and 550 ppm (C) of reductant in N_2 as balance. The total gas flow was 0.25 L min^{-1} NTP and the amount of catalyst was 200 mg, corresponding to a GHSV of 93,000 h^{-1}. The heating rate in TPSR experiments was 10 K min^{-1}. Steady-state activity was measured over the catalytic material with different reactant concentrations.

The reactor outflow was analysed using a set of specific detectors. An Eco Physics CLD 700 AL NO_x chemiluminescence analyser (for NO and total NO_x (NO + NO_2)) allowed the simultaneous detection of NO, NO_2 and NO_x. An Ultramat 6 IR analyser was used to monitor N_2O, and a FID detector was used to follow the total concentration of hydrocarbons (HC). GC–MS analyses were performed on-line using an AGILENT device (GC 6890–MS 5973N) equipped with a CP-PoraBOND Q capillary column (Chrompack, 30 m long, 0.32 mm i.d., 0.5 μm film thickness) with temperature programming from 50 to 280 °C. NIST spectral AGILENT data base was used to identify the detected products.

3.3. Physicochemical characterisations

Transmission electron microscopy was made on a JEOL JEM 100CXII apparatus equipped with a top-entry device,

and operating at 100 kV. X-ray dispersive spectrometry (EDS) was carried out on an AN10000 LINK analyser, equipped with an energy dispersion detector.

4. Existence of cationic sites for TWC over CeO_2-ZrO_2 and Rh/CeO_2-ZrO_2

4.1. Two kinds of metallic active sites for TWC: zero-valent M^0 and cationic M^{x+}

Two kinds of metallic active sites have to be first defined: cationic and zerovalent metallic ones. Let us recall what happens, more particularly, when the support is reducible (case of CeO_2-ZrO_2). The first type of sites can form, through either (i) the reduction of the support (v)–Ce^{3+}–(v), or (ii) a strong metal–support interaction (v)–Rh^{+}–(v)/CeO_2 (Scheme 1), both linked to adjacent oxygen vacancies (v) of the reducible support. In the case of a zeolite, a surface transition metal (TM) complex is formed. The second kind of sites corresponds to accessible supported-zerovalent noble metal atoms. These two kinds of sites are involved in three-way catalysts (TWC).

Formation of M^{x+} on a reducible support. In a previous work, Fajardie et al. [11] have compared the reduction of NO by CO, over both a reducible support alone, –ceria or ceria–zirconia–, and a 0.35 wt.% Rh/CeO_2(75)-ZrO_2(25) catalyst. They have shown that $Ce^{IV+}_{lattice}$ and Rh^{x+}/CeO_2-ZrO_2 are able to reduce NO to N_2 and, simultaneously, to transform CO to CO_2 (Fig. 1b). The Rh^{x+} cation was considered as stabilised in a cationic vacancy at the surface of the reducible support (Scheme 1). This is quite comparable to the Ce^{x+} active sites defined by Soria and coworkers [25,26] on CeO_2. Let us note that a treatment by hydrogen of 0.35 wt.% Rh/CeO_2(75)-ZrO_2(25) did not permit to reduce the rhodium species [11].

4.2. NO adsorbs as a ligand without dissociation on M^{x+}, but dissociates over M^0

Associative adsorption of NO over M^{x+}. Fig. 1a shows that NO has not been dissociated over Rh^{x+}/CeO_2-ZrO_2, as it desorbs under a flowing mixture (CO–O_2 (1.5 vol.% CO+0.65 vol.% O_2+He (concentrations equivalent to TWC conditions))) at about 200 °C. Simultaneously, the reaction CO/O_2 takes place (Fig. 1a). NO acts as a ligand on the "Rh^{x+} species", at a temperature quite lower, compared to that observed on the support alone (about 320 °C, Fig. 1b). This desorption can be used to titrate the "Rh^{x+} species" [12]. This "ligand behaviour" is quite common over cations, as it will be seen later on oxidised metals or reducible supports. The same phenomena occur during the TWC reaction (Fig. 1b): NO desorbs (A–B), simultaneously with the CO oxidation by O_2 (A–C). Once all oxygen has been consumed, in "C", NO reacts and the CO/NO reaction takes place (B, C–D).

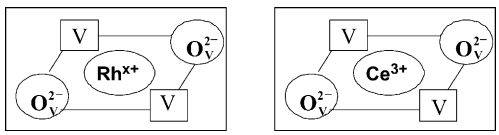

Scheme 1. Cationic sites on CeO_2 or $CeZrO_2$ reducible supports.

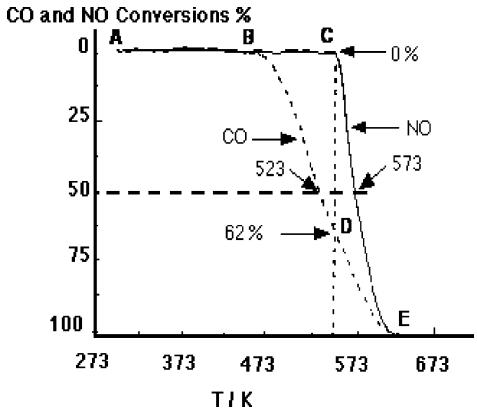

Fig. 2. Rh^0/CeO_2: TPD of NO under a flowing mixture (1.5 vol.% CO + 0.65 vol.% O_2 + He (concentrations equivalent to TWC conditions), 180 °C h^{-1}, 5 L h^{-1}) [27]. The catalyst has been previously pre-treated by TPSR in the stoichiometric (CO/NO/O_2) mixture, before NO adsorption at room temperature.

NO dissociation over M^0. Previous studies on NO chemisorption lead to some clear conclusions on dissociative adsorption of NO. Burch et al. [20] found that nitric oxide dissociates on reduced platinum sites. Root et al. [22] found that NO on Rh(1 1 1) dissociates between 273 and 323 K. Leclercq et al. [23], Cho et al. [24] also assumed NO dissociation through two elementary steps over reduced Pt or Rh, according to Table 1.

The following experiment confirms these data. After calcination of CeO_2 at high temperature, and impregnation, by $RhCl_3$, of the resulting low surface area oxide, a subsequent reduction of the material leads to Rh^0/CeO_2. This catalyst only presents Rh^0 active sites, as shown by benzene hydrogenation [12] (the Rh^{x+} turnover rate of benzene hydrogenation is very low [29]). Fig. 2 shows that no NO desorption peak appears during the whole TWC reaction, on the contrary of what happens on Rh^{x+} catalysts (Fig. 1b). It means that NO dissociates, leaving adsorbed oxygen atoms (*O) on the surface of Rh^0, according to Table 1.

4.3. Kinetics of the CO/NO reaction over M^0 and M^{x+} [19]

This reaction occurs in the TWC process, once the oxygen of the stoichiometric mixture has been consumed (Fig. 1b, at "C"). It corresponds to 87% CO conversion.

Let us consider the cases of Rh^0/SiO_2 and Rh^{x+}/CeO_2-ZrO_2 to give evidence of the difference of behaviour between the two kinds of sites. As can be expected, Manuel et al. [19] had shown that the global kinetic laws over Rh^0 and Rh^{x+} are quite different in the CO/NO reaction.

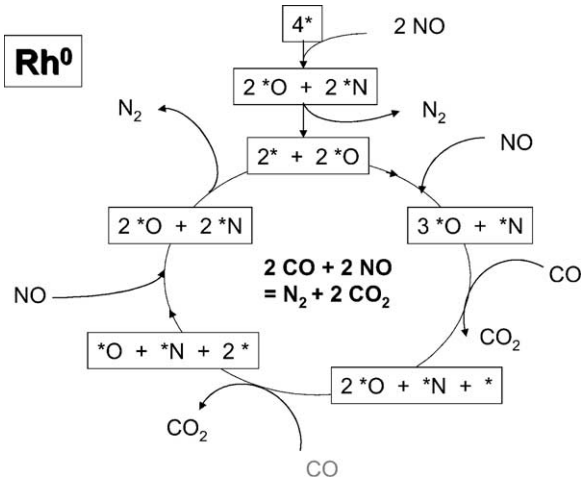

Fig. 3. Catalytic cycle corresponding to the CO/NO reaction over Rh^0 [19,28].

For Rh^0, $r = k_1[CO]^{0.3}[NO]^{-0.6}$, whereas for Rh^{x+}, $r = k_2[CO]^{0.4}[NO]^{+0.6}$. It means that in the last case (positive order with respect to NO) there is no competitive adsorption between CO and NO, whereas it is the case for Rh^0 (negative order in respect to NO).

Catalytic cycle for the CO/NO reaction over Rh^0 [19]. Fig. 3 shows the catalytic cycle which turns over at high temperature, when no more N_2O is produced. When there are two adjacent free sites when NO sticks to the surface, NO dissociates. If it is not the case, then NO can adsorb linearly, with the possibility of producing N_2O which can leave the cycle: this generally happens at a temperature lower than the temperature of light-off of reactants. There is a kinetic coupling, in the same cycle, between the dissociation of NO, leading to the formation of N_2, and the CO oxidation to CO_2, leading to the scavenging of the *O species left by the NO dissociation, and restoring the active sites.

The kinetics and modelling of this reaction has been done by Manuel et al. [19,28].

Catalytic cycle for CO/NO reaction over Rh^{x+} [15,19]. Fig. 4 shows the corresponding catalytic cycle. It works like homogeneous supported catalysis, where NO and CO act as ligands. As a consequence, the whole reaction occurs on a unique site, and the two reactants are no more in competition. Therefore, both orders of reaction are positive. The detailed kinetics and simulation have been done by Manuel et al. [19,28].

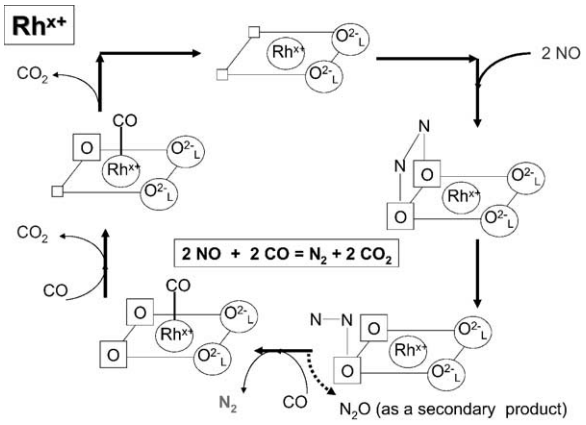

Fig. 4. Catalytic cycle corresponding to TWC over Rh^{x+} [15,19,28].

5. Link between the TPD of NO, and the TWC and deNO$_x$ processes

5.1. Case of TWC: comparison between CeO_2-ZrO_2 alone and Rh^{x+}/CeO_2-ZrO_2 in the reduction of NO by CO (Fig. 1a and b)

Fajardie et al. [11] have given evidence for the following four points during the TWC process (Fig. 1b):

(i) On both the support alone, and Rh^{x+}/CeO_2-ZrO_2, NO is not dissociated and desorbs during TPSR; the phenomenon occurs according to the same process, on both "metal cationic species", and Ce^{3+}. This last one is able to proceed to the TWC process, but at a quite higher temperature.

(ii) The catalytic effect of Rh^{x+} leads to a quite lower temperature of NO desorption (200 °C) compared to that over the support alone (320 °C).

(iii) The desorption occurs, during the reaction, when flowing a complete CO/NO/O_2 mixture, simultaneously with the CO activation and oxidation, i.e. at the temperature where TWC occurs.

(iv) The temperature of the reaction is exactly the same as that observed during the TPD of NO under flowing CO/O_2 mixture (Fig. 1a).

As a conclusion, the desorption of NO during the TPD experiment is indicative of the temperature of the TWC process. This result, as shown hereafter, is quite general and can be extrapolated to deNO$_x$ catalysts. Furthermore, TWC can occur over either M^0 or M^{x+} active sites.

5.2. Case of deNO$_x$ catalysts: example of PdCo/HMOR, with methane as a reductant Berger et al. [13,21]

Fig. 5 shows both the TPD of NO pre-adsorbed at room temperature (Fig. 5a) and the TPSR plot of the deNO$_x$ reaction over PdCo/HMOR (Fig. 5b). Experimental details are reported in the caption of Fig. 5.

Desorption of NO (Fig. 5a, zones 1 and 2). The TPD plot (Fig. 5a) shows that there are two sites for the adsorption of NO, which then suffers two desorptions, either with the production of N_2 and NO (first peak at about 100 °C), or with the formation of N_2, N_2O and NO (second peak at about 250–360 °C). Let us note the presence of N_2O during this TPD process. More particularly also note the simultaneous dissociation and formation of N_2: the simultaneity of these events shows that when NO is activated, part of it

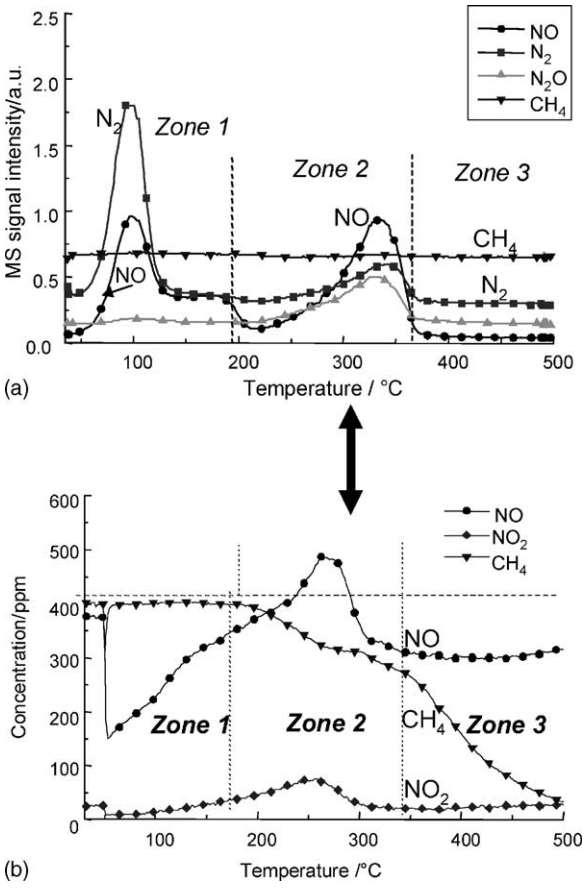

Fig. 5. In zone 2, the same temperature (200 °C, activation temperature of NO) is observed for both the TPD of NO (a) and the temperature of deNO$_x$ reaction (b). Part (a) shows pre-adsorption of NO at room temperature over Co-Pd/H-mordenite (Gaz de France-IRMA catalyst) pre-treated in flowing Ar up to 500 °C in order to get only Co^{2+} species exchanged in HMOR (1000 ppm NO in He (50 cm^3 min^{-1}, for 90 min)). TPD: 1000 ppm CH_4 in He, 10 K min^{-1} (note that methane does not react) in these conditions. Part (b) shows TPSR profile of the deNO$_x$ reaction in the presence of methane, over CoPd/HMOR pre-treated in air. Feed: 400 ppm NO + 400 ppm CH_4 + 5 vol.% O_2, VVH = 62,000 h^{-1}.

is desorbing, and the reduction of NO is already occurring (without release of dioxygen as controlled by GC–MS); N_2O appears as the intermediate of the NO reduction. Its formation is indicated on the catalytic cycle of Fig. 4.

Reduction of NO. The previous second peak (Fig. 5a, zone 2) corresponds to the temperature window of the reduction of NO during the TPSR (Fig. 5b, zone 2).

Oxidation of NO to NO_2 (Fig. 5b, zones 1 and 2). In the deNO$_x$ conditions, NO transforms to NO_2. But it must be noted that in zone 2, at about 255 °C, NO_2 is more consumed than produced. This consumption is concerted with the consumption of methane and the reduction of NO.

Consumption (oxidation) of methane (Fig. 5b, zones 2 and 3). Methane suffers a mild oxidation by NO_2, and there is simultaneously a total oxidation of methane to CO_2 (not reported here) [30]; NO is simultaneously reduced to N_2 as detected by chromatography [30]. Berger et al. [13,21] have demonstrated that the mild oxidation of methane leads to the production of methanol and formaldehyde, as detected by GC–MS during the TPSR. They are the "activated" species of methane and the effective reductants for the reduction of NO.

Existence of three catalytic functions, and concerted actions between the corresponding three catalytic cycles. Berger et al. [13,21] have shown that three functions are necessary for the deNO$_x$ process to occur:

(i) oxidation of NO to NO_2;
(ii) mild oxidation of methane to alcohol and aldehyde, in the presence of NO_2;
(iii) reduction of NO to N_2, assisted by the deep oxidation of the alcohol and aldehyde to CO_2.

Simultaneously the active site of the third function is regenerated. Fig. 6 shows the three catalytic cycles which have to turn over simultaneously in order for the deNO$_x$ reaction to occur. Cycle 1 provides NO_2 to cycle 2; cycle 2 delivers the active HC_xO_y oxidised species to cycle 3, in order to proceed to the decomposition–reduction of NO to N_2. The HC_xO_y species are simultaneously transformed to CO_2 and H_2O. The detailed process has been described by Berger et al. [13,21].

The interaction between NO_2 and HC is clearly located in the second catalytic cycle. Baudin et al. have detected RNO_x and shown the decomposition of RNO_x to $C_xH_yO_z$ over a Ir/CeZrO$_2$ catalyst [34]. The dinitrogen is formed in the last cycle and is not linked to any organo–nitro compound.

In summary, the previous transient experiments and catalytic cycles lead to a model of the NO reduction assisted by the oxidation of a pre-activated HC_xO_y (lean conditions), without kinetic coupling between catalytic sequences.

5.3. Evidence for HC_xO_y as efficient reductants in the third catalytic cycle [14,31]

If the preceding model is right, substituting HC by the corresponding alcohol (propene by propanol in the present case), and designing a catalyst with only the third function (Rh^{x+} in the example), a deNO$_x$ process must be observed.

Gorce et al. [14,31]. have extrapolated the model to a 0.4 wt.% Rh/CeZrO$_2$ simplified catalyst. Fig. 7 shows all the characteristics described in the model: simultaneous activation of propanol with the deNO$_x$ reaction, leading to 44% NO_x conversion at 300 °C. Let us note that the deNO$_x$ process occurs at the same temperature as for propene, which is due to the fact that the "activation" of NO occurs at the same temperature [14].

6. Non-thermal plasma assisted catalytic deNO$_x$

Non-thermal plasma assisted catalytic NO_x remediation completely enters the model: the plasma reactor substitutes functions 1 and 2, and provides the HC_xO_y species to a "third-function" catalyst [31]. These evaluations were

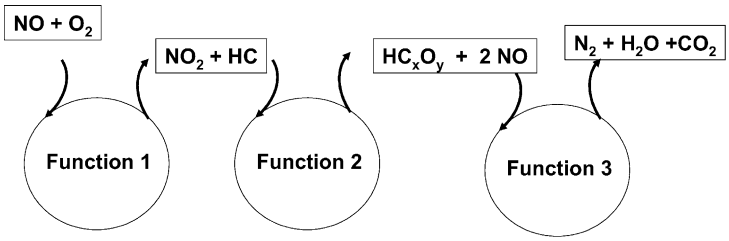

Fig. 6. Scheme for the three-function catalyst. Concerted action for the selective reduction of NO by hydrocarbons (HC). HC_xO_y: partially oxidised HC.

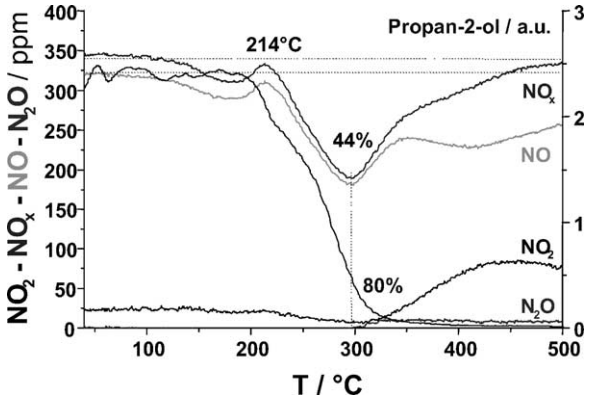

Fig. 7. $deNO_x$ reaction over $Rh^{x+}/CeZrO_2$ in the presence of propanol [14,31] (6000 ppm C_3H_7OH, 340 ppm NO; 8 vol.% O_2).

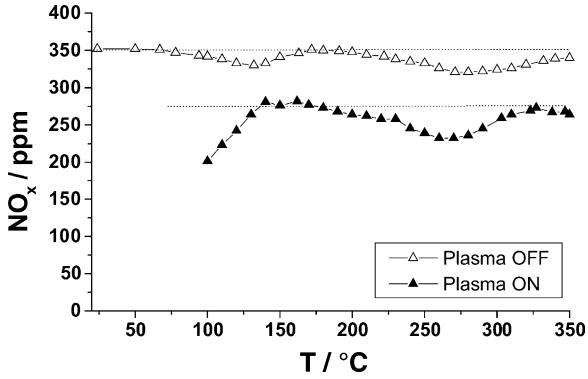

Fig. 9. Plasma assisted experiment over 0.4 wt.% Rh/CeO_2-ZrO_2, a "simplified catalyst" presenting only the third function.

made either in the absence or in the presence of a cylindrical DBD non-thermal plasma reactor (36 J L^{-1}) (Fig. 8) over $Rh^{x+}/CeZrO_2$ simplified catalyst (major third function alone). Both temperature programmed surface reaction (TPSR, 1 K min^{-1}) and isothermal reactions were performed (340 ppmv NO, 1900 ppmv C_3H_6, 8 vol.% O_2 in N_2, 45,000 h^{-1}).

Composition of plasma exhaust gases are in agreement with the data of Hoard and Balmer [32], and Doraï and Kushner [33]. More particularly, HC_xO_y (CH_2O, CH_2O_2, CH_3OH, etc.), NO_2, organo–nitro compounds "R–NO_x" (CH_3ONO_2, etc.) were detected. Fig. 9 suggests an advantageous plasma-catalyst coupling effect on the NO_x remediation which is in full accordance with the proposed model: $deNO_x$ conversion was 8% without plasma and 34% NO_x remediation were observed plasma "on".

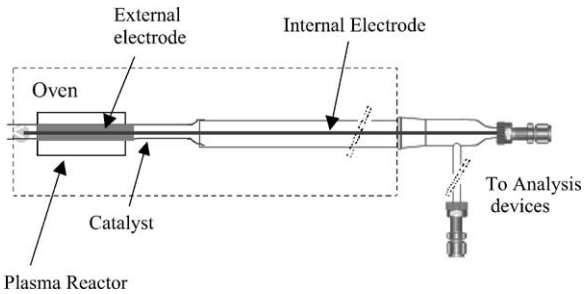

Fig. 8. Plasma and associated catalytic reactors. Inner electrode: tungsten wire (0.9 mm Ø); outer electrode: aluminium foil (13 mm Ø); plasma reactor volume: 16 cm^3; high voltage power supply (pulse generator); energy deposition: 35 mJ $pulse^{-1}$.

7. Conclusion

One of the characteristics of NO reduction, in either stoichiometric or lean conditions, is that the domain of temperature where the reaction occurs can be predicted by the temperature of activation of NO, i.e. its temperature of desorption. A second feature which seems to be able to gather all previous works, is that a given catalyst can present transition metal cations, mainly due to a strong metal–support interaction (for reducible supports or alumina, etc.), or to exchange process (case of zeolites).

If we assumed, with literature data, that NO dissociates over a zero-valent metal, whereas it associatively adsorbs as a ligand on a metal cation, we observed that: (i) for TWC process, the reaction occurs over both M^0 and M^{x+}. (ii) In the case of $deNO_x$ reaction (lean conditions), the metal cation is the site where the NO decomposition occurs, going to the dinitrogen formation through N_2O intermediate. Depending on the nature of the cation and temperature, N_2O can desorb or transform to N_2 depending on the set of rate constants [16].

For $deNO_x$ global reaction, temperature programmed desorptions and reactions lead to the conclusion that effective reductants of NO are oxidised hydrocarbon species (HC_xO_y), such as alcohols or aldehydes. The oxidation of

HC can follow two routes: total oxidation, or mild oxidation to HC_xO_y compounds. NO_2 has been observed to favour this second route. Therefore, a three-function catalyst design will lead to a complete and efficient catalytic material. Three catalytic cycles have to turn over simultaneously: oxidation of NO to NO_2, mild oxidation of HC to HC_xO_y, decomposition–reduction of NO with total oxidation of HC_xO_y species and recovering of the free active site. They are not kinetically coupled as they have no common adsorbed species [16,17], but they must work in a concerted way.

Acknowledgements

C. Potvin, J.M. Manoli, H. Pernot, C. Thomas, M. Berger, O. Gorce, I. Manuel, from LRS, and Engineers from ADEME, Gaz de France, PSA-Peugeot Citroën, Renault, Rhodia are greatly acknowledged for participating to the model and financial supports.

References

[1] V.I. Parvulescu, P. Grange, B. Delmon, Catal. Today 46 (1998) 233.
[2] M.D. Amiridis, T.J. Zhang, R.J. Farrauto, Appl. Catal. B 10 (1996) 203.
[3] A. Fritz, V. Pitchon, Appl. Catal. B 13 (1997) 1.
[4] R. Burch, J.P. Breen, F.C. Meunier, Appl. Catal. B 39 (2002) 283.
[5] C.H.F. Peden, D.W. Goodman, D.S. Blair, P.J. Berlowitz, G.B. Fisher, S.H. Oh, J. Phys. Chem. 92 (1988) 1563.
[6] N.W. Cant, W.K. Hall, J. Catal. 54 (1978) 372.
[7] S.H. Oh, C.C. Eickel, J. Catal. 128 (1991) 526.
[8] Y. Yu, J. Catal. 87 (1984) 152.
[9] T. Bunluesin, H. Cordatos, R.J. Gorte, J. Catal. 157 (1995) 222.
[10] S.H. Oh, Eickel, J. Catal. 112 (1988) 543.
[11] F. Fajardie, J.-F. Tempère, J.-M. Manoli, O. Touret, G. Blanchard, G. Djéga-Mariadassou, J. Catal. 179 (1998) 469.
[12] L. Salin, C. Potvin, J.-F. Tempère, M. Boudart, G. Djéga-Mariadassou, J.-M. Bart, Ind. Eng. Chem. Res. 37 (1998) 4531.
[13] M. Berger, Doctoral Thesis, Université Pierre et Marie Curie, Paris, 2000.
[14] O. Gorce, Doctoral Thesis, Université Pierre et Marie Curie, Paris, 2001.
[15] G. Djéga-Mariadassou, F. Fajardie, J.-F. Tempère, J.-M. Manoli, O. Touret, G. Blanchard, J. Mol. Catal. A 161 (2000) 179.
[16] M. Boudart, G. Djéga-Mariadassou, Cinétique des Réactions en Catalyse Hétérogène, Masson, Paris, 1982;
M. Boudart, G. Djéga-Mariadassou, Kinetics of Heterogeneous Catalytic Reactions, Princeton University Press, Princeton, NJ, 1984.
[17] G. Djéga-Mariadassou, M. Boudart, J. Catal. 216 (2003) 89.
[18] F. Jayat, C. Lembacher, U. Schubert, J.A. Martens, Appl. Catal. B 21 (1999) 221.
[19] I. Manuel, C. Thomas, C. Bourgeois, H. Colas, N. Matthess, G. Djéga-Mariadassou, Catal. Lett. 77 (2001) 193;
I. Manuel, C. Thomas, H. Colas, N. Matthess, G. Djéga-Mariadassou, Top. Catal., in press.
[20] R. Burch, P.J. Millington, A.P. Walker, Appl. Catal. B 4 (1994) 65.
[21] M. Berger, H. Lauron-Pernot, E. Tena, G. Djéga-Mariadassou, J. Mol. Catal., 2004, to be published.
[22] T.N. Root, L.D. Schmidt, G.B. Fisher, Surf. Sci. 150 (1985) 173.
[23] G. Leclercq, C. Dathy, G. Mabilon, L. Leclercq, in: A. Crucq (Ed.), Catalysis and Automotive Pollution Control II, vol. 71, Elsevier, Amsterdam, 1991, p. 181.
[24] B.K. Cho, B.H. Shanks, J.E. Bailey, J. Catal. 115 (1989) 486.
[25] A. Martinez-Arias, J. Soria, J.C. Conesa, X.L. Seoane, A. Arcoya, R. Cataluna, J. Chem. Soc., Faraday Trans. 91 (11) (1995) 1679.
[26] R. Cataluna, A. Arcoya, X.L. Seoane, A. Martinez-Arias, J.M. Coronado, J.C. Conesa, J. Soria, L.A. Petrov, in: A. Frennet, J.M. Bastin (Eds.), Catalysis and Automotive Pollution Control III, vol. 96, Elsevier, Amsterdam, 1995, p. 215.
[27] F. Fajardie, Doctoral Thesis, Université Pierre et Marie Curie, Paris, 1996.
[28] I. Manuel, Doctoral Thesis, Université Pierre et Marie Curie, Paris, 2002.
[29] F. Fajardie, J.-F. Tempère, G. Djéga-Mariadassou, G. Blanchard, J. Catal. 163 (1996) 77.
[30] J.W. Park, Doctoral Thesis, Université Pierre et Marie Curie, Paris, 2004, to be published.
[31] O. Gorce, H. Jurado, C. Thomas, G. Djéga-Mariadassou, A. Khacef, J.M. Cormier, J.M. Pouvesle, G. Blanchard, S. Calvo, Y. Lendresse, SAE Technical Paper Series 2001-01, 2001, p. 3508.
[32] J. Hoard, M.L. Balmer, SAE Technical Paper Series 1998-01, 1998, p. 2429.
[33] R. Doraï, M.J. Kushner, SAE Technical Paper Series 1999-01, 1999, p. 3683.
[34] F. Baudin, C. Thomas, P. Da Costa, Y. Lendresse, S. Schneider, P. Rouveyrolles, G. Plassat, G. Djéga-Mariadassou, Top. Catal., in press.